available at www.sciencedirect.com

ScienceDirect

journal homepage: www.elsevier.com/locate/biochempharm

The metabolomics of (±)-arecoline 1-oxide in the mouse and its formation by human flavin-containing monooxygenases

Sarbani Giri [a,b], *Kristopher W. Krausz* [a], *Jeffrey R. Idle* [c], *Frank J. Gonzalez* [a,*]

[a] *Laboratory of Metabolism, Center for Cancer Research, National Cancer Institute, National Institutes of Health, Bethesda, MD 20892, United States*

[b] *Department of Life Science, Assam University, Silchar 788011, Assam, India*

[c] *Institute of Pharmacology, 1st Faculty of Medicine, Charles University, 128 00 Praha 2, Czech Republic*

ARTICLE INFO

Article history:
Received 30 August 2006
Accepted 16 October 2006

Keywords:
Arecoline
Metabolomics
Flavin-containing monooxygenase
Ultra-performance liquid chromatography
Tandem mass spectrometry
Coupled time-of-flight mass spectrometry

ABSTRACT

The alkaloid arecoline is a main constituent of areca nuts that are chewed by approximately 600 million persons worldwide. A principal metabolite of arecoline is arecoline 1-oxide whose metabolism has been poorly studied. To redress this, synthetic (±)-arecoline 1-oxide was administered to mice (20 mg/kg p.o.) and a metabolomic study performed on 0–12 h urine using ultra-performance liquid chromatography-coupled time-of-flight mass spectrometry (UPLC-TOFMS) with multivariate data analysis. A total of 16 mass/retention time pairs yielded 13 metabolites of (±)-arecoline 1-oxide, most of them novel. Identity of metabolites was confirmed by tandem mass spectrometry. The principal pathways of metabolism of (±)-arecoline 1-oxide were mercapturic acid formation, with catabolism to mercaptan and methylmercaptan metabolites, apparent C=C double-bond reduction, carboxylic acid reduction to the aldehyde (a novel pathway in mammals), *N*-oxide reduction, and de-esterification. Relative percentages of metabolites were determined directly from the metabolomic data. Approximately, 50% of the urinary metabolites corresponded to unchanged (±)-arecoline 1-oxide, 25% to other *N*-oxide metabolites, while approximately, 30% corresponded to mercapturic acids or their metabolites. Many metabolites, principally mercapturic acids and their derivatives, were excreted as diastereomers that could be resolved by UPLC-TOFMS. Arecoline was converted to arecoline 1-oxide *in vitro* by human flavin-containing monooxygenases FMO1 (K_M: 13.6 ± 4.9 μM; V_{MAX}: 0.114 ± 0.01 nmol min^{-1} μg^{-1} protein) and FMO3 (K_M: 44.5 ± 8.0 μM; V_{MAX}: 0.014 ± 0.001 nmol min^{-1} μg^{-1} protein), but not by FMO5 or any of 11 human cytochromes P450. This report underscores the power of metabolomics in drug metabolite mining.

1. Introduction

It has been estimated that areca nut chewing is the fourth most popular habit worldwide, after the use of tobacco, alcohol and caffeine, with 600 million users [1,2]. The major alkaloids present in areca nut are arecoline, arecaidine, guvacine and guvacoline [3]. There are several different ways in which areca nut is consumed in India, Taiwan and South East Asia, but areca nut chewing is the most common and manifests several pharmacological effects, including euphoria, central nervous system stimulation, vertigo, salivation, miosis, tremor and bradycardia [3]. There have been epidemiological studies

* *Corresponding author at*: Laboratory of Metabolism, Center for Cancer Research, National Cancer Institute, Building 37, Room 3106, Bethesda, MD 20892, United States. Tel.: +1 301 496 9067; fax: +1 301 496 8419.
E-mail address: fjgonz@helix.nih.gov (F.J. Gonzalez).

0006-2952/$ – see front matter © 2006 Published by Elsevier Inc.
doi:10.1016/j.bcp.2006.10.017

carried out in India, Pakistan, Taiwan and China that reported associations between areca nut chewing with oral precancerous lesions, specifically submucous fibrosis and leukoplakia [3,4]. The habitual chewing of areca nut is proposed to be deleterious to human health, especially in relation to the risk of the development of oral cancer [3,5]. The role of the areca alkaloids, such as arecoline, in the adverse health effects of areca nut chewing is not known.

We have recently reported on a study in which arecoline and arecaidine were administered to mice and their urinary metabolite profiles revealed using ultra-performance liquid chromatography-coupled time-of-flight mass spectrometry (UPLC-TOFMS) and metabolomic analyses [6]. Eleven urinary metabolites of arecoline were identified, the major two of which were arecoline 1-oxide, which had been previously reported [7,8], and the novel metabolite *N*-methylnipecotic acid [6], the result of C=C double-bond reduction. In the only previous report, administration of arecoline 1-oxide to rats was said to produce a broadly similar metabolic picture as arecoline itself, and the author stated that this was evidence for the reduction of arecoline 1-oxide back to arecoline and then its subsequent metabolism [8]. This process of *N*-oxide reduction and re-synthesis has been termed "metabolic retroversion" from the study of trimethylamine *N*-oxide in volunteers with a trimethylamine *N*-oxidation pharmacogenetic deficiency [9].

The enzymology of arecoline conversion to its principal metabolite arecoline 1-oxide has not been reported. It is not known whether arecoline 1-oxide is formed by a flavin-containing monooxygenase (FMO) or by one or more cytochromes P450 (P450). In addition, the metabolites of arecoline 1-oxide have not been studied in detail. These issues are important because one or more metabolites of arecoline may be responsible for the human toxicity profile associated with areca nut chewing habits.

The flavin-containing monooxygenases (EC 1.14.13.8) catalyze the NADPH-dependent oxidation of a variety of xenobiotics which contain nucleophilic heteroatoms, typically nitrogen, sulfur or phosphorus [10]. The FMOs are efficient two-electron oxygenating enzymes for *N*-oxidation, unlike P450s, which generally use sequential one-electron transfer chemistry [11]. The microsomal FMO enzyme family is comprised of five isozymes, FMO1–FMO5 whose expression is tissue-specific [12,13]. FMO1 is predominantly expressed in human kidney, and FMO2 in lung and kidney [13]. FMO3 is the prominent isozyme in adult human liver, FMO4 is more broadly distributed in liver, kidney, small intestine and lung, and FMO5 is expressed in human liver, lung, small intestine and kidney [13].

We report here a study in which we have harnessed the resolving power of UPLC, the accurate mass determination of TOFMS and metabolomic data analysis to investigate the urinary metabolic products of (±)-arecoline 1-oxide (Fig. 1) when administered to mice. In addition, we report an investigation of the potential human enzymes that may carry out the *N*-oxidation of arecoline.

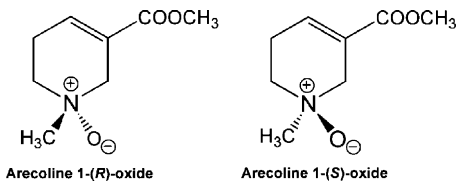

Fig. 1 – Absolute configurations of arecoline 1-(*R*)-oxide and 1-(*S*)-oxide.

2. Materials and methods

2.1. Materials

(±)-Arecoline 1-oxide was synthesized from arecoline hydrobromide and peroxyacetic acid as previously described [6,8]. The racemic nature of the product was additionally confirmed by polarimetry ($[\alpha]_D^{23} = +0.02$). Arecoline hydrobromide, methimazole, caffeine, and NADPH were purchased from Sigma–Aldrich (St. Louis, MO). All solvents and inorganic reagents were of the highest grade commercially available. Recombinant human P450 and FMO isozymes and P450 insect control microsomes were obtained from BD Biosciences (Woburn, MA).

2.2. Animals and treatments

Mice used were 6 to 7-week-old FVB males. Mice were maintained under standard 12 h light/12 h dark cycle with water and chow provided *ad libitum*. Handling was in accordance with an animal study protocol approved by the National Cancer Institute Animal Care and Use Committee. (±)-Arecoline 1-oxide (20 mg/kg) was administered by gavage to six mice and urine (0–12 h) collected from mice housed individually in glass metabolic chambers (Jencons, Leighton Buzzard, UK). This dose was chosen because it is 20% of the LD50 value for arecoline [14]. Pre-dose control 0–2 h urines were similarly collected from each mouse, at least 12 h prior to arecoline administration.

2.3. Incubations with recombinant human P450s

Incubations with a panel of cytochromes P450 were carried out in 100 mM tris–HCl, pH 7.4, containing 2 pmol of each of the cDNA expressed P450 enzymes (insect control, CYP1A1, CYP1A2, CYP1B1, CYP2A6, CYP2B6, CYP2C9, CYP2C19, CYP2D6, CYP2E1, CYP3A4, and CYP4A11), together with 50 μM of arecoline in a final volume of 200 μl. After 3 min pre-incubation at 37 °C, the reaction was initiated by the addition of 50 μl of 10 mM NADPH and continued for 20 min in shaking water bath at 37 °C. The reactions were terminated by cooling on ice and the addition of 10 μl of 20% perchloric acid. Caffeine (5 μl) with a final concentration of 50 μM was used as internal standard. The reaction mixture was centrifuged at 14,000 × *g* for 15 min. The supernatants were diluted with 2 vol. of water and placed in autoinjector vials for analysis by UPLC-TOFMS.

2.4. Incubations with recombinant human FMO isozymes

Each incubation reaction was carried out in 50 mM potassium phosphate buffer, pH 7.9, with FMO1, FMO3 and FMO5 (200 μg/ml protein) to a final volume of 200 μl. After 3 min pre-incubation at 37 °C, the reaction was initiated by the addition of 10 mM NADPH. Incubations were carried out for 20 min and then the reactions were terminated by cooling on ice and the

addition of 10 μl of 20% perchloric acid. These reaction conditions were established to be linear with respect to enzyme content and incubation time. The mixture was vortexed for 20 s and then centrifuged at 14,000 × *g* for 15 min. The supernatants were diluted with 2 vol. water and placed in autoinjector vials for analysis by UPLC-TOFMS. The kinetics of arecoline *N*-oxidation by human FMO1 and FMO3 were determined by incubating arecoline in duplicate at six concentrations (5, 10, 25, 50, 100 and 200 μM). Incubations were carried out at different protein concentrations (5, 10, 20, 50, 100 and 200 $\mu g\,ml^{-1}$ FMO) and with 50 μM arecoline. Enzyme activity was expressed as $\mu mol\,min^{-1}\,\mu g^{-1}$ FMO. Incubations were carried out with FMO1 and FMO3 with arecoline (50 μM) and the FMO substrate/inhibitor methimazole (10, 100, 200 and 1000 μM) [15]. In all reactions, caffeine (50 μM) was used as internal standard.

2.5. UPLC-TOFMS analysis

Batches of pre-dose and post-dose urines were analyzed together by UPLC-TOFMS [16]. Urine samples were mixed with the equal volume of water and centrifuged at 14,000 rpm to remove particles and protein. A 200 μl aliquot of the supernatant was transferred to an auto-sampler vial for UPLC-TOFMS analysis. Urine samples (5 μl/injection) were separated on a 50 mm × 2.1 mm ACQUITY™ 1.7 μm C_{18} column (Waters Corp, Milford, MA) using an ACQUITY™ UPLC system (Waters) with a gradient mobile phase comprised of 0.1% formic acid (A) and acetonitrile containing 0.1% formic acid (B). A 0.6 ml min^{-1} flow rate was maintained in a 10 min run. The gradient comprised 100% A for 0.5 min, increasing to 100% B over the next 8.5 min. The eluent was directly introduced into the mass spectrometer by electrospray. Mass spectrometry was performed on a Waters Q-TOF Premier™ operating in positive ion mode. The desolvation gas flow was set to 600 l h^{-1} at a temperature of 350 °C with the cone gas set to 50 l h^{-1} and the source temperature set to 120 °C. The capillary voltage and the cone voltage were set to 3000 and 30 V, respectively. Leucine-enkephalin was used as the lock mass (*m*/*z* 556.2771) for accurate mass calibration and introduced using the LockSpray™ interface at 30 μl min^{-1} and a concentration of 0.2 ng μl^{-1} in 50% aqueous acetonitrile containing 0.1% formic acid. In MS scanning, data were acquired in centroid mode from 100 to 950 *m*/*z*. As for MS/MS fragmentation of target ions, collision energy ranging from 15 to 30 V was applied. Following data acquisition, UPLC-MS chromatograms and spectra were further analyzed by MassLynx application software (Waters).

2.6. Data processing and multivariate data analysis (MDA)

Following UPLC-TOFMS data acquisition, centroided and integrated mass chromatographic data were deconvoluted by MarkerLynx™ software (Waters) to generate a multivariate data matrix. The intensity of each ion was calculated as the percentage of total ion counts (TIC) in the whole chromatogram. The data matrix and sample list were further exported into SIMCA-P + ™ software (Umetrics, Kinnelon, NJ) for MDA. PCA and PLS-DA were conducted after data were transformed by mean-centering and Pareto optimization, a scaling technique that increases the importance of low concentration metabolites without significant amplification of noise. Different to unsupervised PCA, samples/observations were classified as the group of control and arecoline-treated in PLS-DA. After PCA and PLS-DA processing, principal components were generated to highlight the major latent variables in the data matrix and were described in a scattering plot. Identification of potential arecoline metabolites were further performed by analyzing the loadings plot and contribution table.

2.7. Identification of metabolites

PCA analysis reveals the ions that contribute most significantly to the group differences, for example, arecoline 1-oxide treated urines versus pre-treatment urines. In general, the 20 most significant ions were examined in more detail. These were expected to be metabolites of arecoline 1-oxide, or alternatively, endogenous compounds whose levels were elevated by the administration of arecoline 1-oxide. Elemental compositions of each of the ions were generated by MarkerLynx and those with best fits, and also C, H, N, O, and S compositions that could be related to arecoline 1-oxide, were noted. In all cases, the identity of the metabolite was apparent from its elemental composition. In the instances where *N*-oxides were proposed as metabolites, experiments were carried out with $TiCl_3$ reduction, which is specific for *N*-oxides [6,17], to confirm that the ion in question disappeared after this treatment. However, no authentic standards existed for most of the proposed metabolites identified. Therefore, MS/MS experiments were performed to confirm or refute proposed chemical structures.

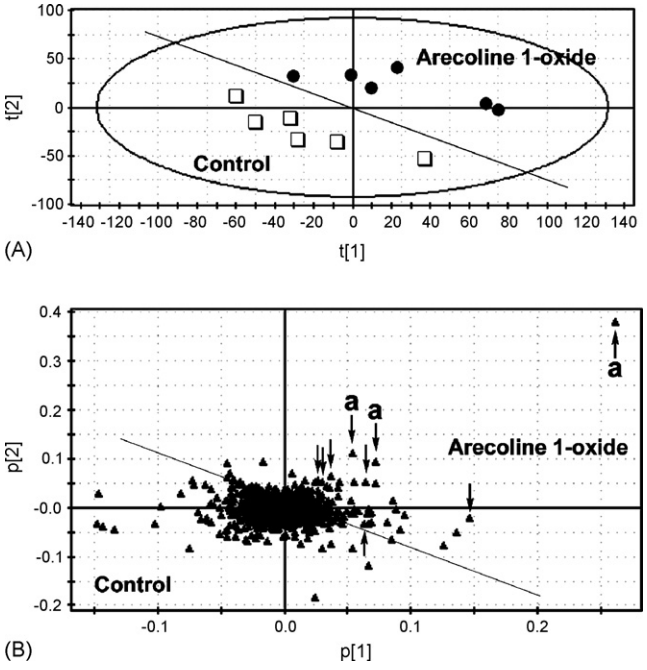

Fig. 2 – PCA scores plot showing group separation for urines from control and arecoline 1-oxide treated animals (A) and the corresponding PCA loadings plot (B). Arrows represent ions identified as arecoline 1-oxide metabolites. Three ions deriving from the parent compound are also marked with "a".

Table 1 – Identification of metabolites of arecoline 1-oxide (20 mg/kg p.o.) in mouse urine by UPLC-TOFMS and metabolomic analysis of ion-retention time pairs

Metabolite number	Mass (MH^+)	Retention time (min)	Deduced formula (M)	Error (ppm)	Identity	Score[a]	Peak[b] area (mean ± S.D.)
I	172.096	1.12–1.13	$C_8H_{13}NO_3$	4.6–6.1	Arecoline 1-oxide	41.9	1630 ± 858
	343.184				(dimer) (+1 isotope)	11.9	125 ± 31.4
	173.102					9.9	
IIa	335.126	1.97	$C_{13}H_{22}N_2O_6S$	1.2	Arecoline 1-oxide mercapturic	6.7	66.2 ± 25.4
IIb	335.126	1.78	$C_7H_{11}NO$	7.1	acid diasteriomers [1-(R,S) 4-(R,S)]	5.7	
III	126.091	0.58			1-Methyl-3,4,-dehydropiperidine-3-carboxaldehyde	6.4	96.6 ± 50.9
IVa	174.112	3.40	$C_8H_{15}NO_3$	2.9	1-Methylnipecotic acid 1-oxide methyl ester diasteriomers [1-(R,S) 3-(R,S)]	5.8	
IVb	174.112	1.73				4.6	44.6 ± 26.1
Va	190.092	0.82	$C_8H_{15}NO_2S$	7.4	4-Mercapto-1-methylnipecotic acid methyl ester diasteriomers [3-(R,S) 4-(R,S)]	5.8	51.7 ± 27.9
Vb	190.096	1.95				3.1	
Vc	190.107	2.15				2.9	
VI	142.081	0.30	$C_7H_{11}NO_2$	8.4	Arecaidine	4.5	5.9 ± 1.1
VII	220.101	2.38	$C_9H_{17}NO_3S$	2.7	4-Methylmercapto-1-methylnipecotic acid 1-oxide methyl ester diasteriomers [1-(R,S) 3-(R,S) 4-(R,S)]	4.0	14.0 ± 5.9
VIII	156.102	0.64	$C_8H_{13}NO_2$	5.8	Arecoline	3.8	13.0 ± 4.5
IXa	319.133	1.41	$C_{13}H_{22}N_2O_5S$	5.3	Arecoline	3.7	12.5 ± 6.8
IXb	319.133	1.26			Mercapturic acid diasteriomers [3-(R,S) 4-(R,S)]	2.8	

[a] Measure of the contribution of an ion to the group difference between treated and control urines, generated by SIMCA-P+.
[b] Area of the chromatographic peak of extracted exact mass (50 ppm tolerance).

2.8. *Quantitation of metabolites*

The MDA using SIMCA-P+ produced a contributions table that ranked the ions in terms of their contribution to the group difference, i.e., between test and blank urines. From previous experience [6], we are aware that these contribution scores are correlated with the relative quantitative importance of each metabolite. However, in the absence of authentic standards, several assumptions must be made to assure the quantitative nature of this analysis, as follows: (i) that there was little or no fragmentation of the protonated molecular ions under the instrumental conditions employed, (ii) that all compounds of interest ionized to a similar extent and (iii) that ion suppression affected all analytes similarly. Accordingly, therefore, it is appreciated that these estimates of relative excretion of metabolites are approximate.

3. Results

3.1. *Metabolomic analysis of mouse urine after (±)-arecoline 1-oxide administration*

Urines collected 0–12 h after the administration of 20 mg/kg (±)-arecoline 1-oxide were analyzed by UPLC-TOFMS together with blank urines from the same male FVB mice. MVA using unsupervised PCA yielded a clear separation in the scores plot between the six urines from (±)-arecoline 1-oxide-treated mice and the six control urines (Fig. 2A). The corresponding loadings plot revealed the characteristic dense cloud that represented the fractionation by UPLC-TOFMS of the mouse urinary metabolome into some 5000 mass/retention time pairs (Fig. 2B). Clear outliers can be seen in the direction corresponding to the administration of arecoline 1-oxide, i.e., a positive increase in both component 1 (p[1]) and component 2 (p[2]) in the PCA loadings plot (Fig. 2B). Supervised PLS-DA analysis, for which, unlike PCA, the identity of each urine as either test or control is utilized in the analysis, did not improve the separation of groups in the scores plot. Therefore, all determinations of urinary biomarkers associated with arecoline 1-oxide administration were made purely from the PCA data. Table 1 shows 16 mass/retention time pairs that were associated with the administration of arecoline 1-oxide and that had a score value, that is a function of the contribution to the group difference in the scores plot (Fig. 2A), of >2.8. This cut-off point of close to 3 was chosen for reasons that will be discussed below. There were other mass/retention time pairs with scores >3 that are not shown in Fig. 3 because analysis of their empirical formulae revealed that they were unlikely to be metabolites of arecoline 1-oxide. These urinary constituents were perhaps elevated due to the administration of arecoline 1-oxide by as yet undisclosed mechanisms. Similarly, mass/retention time pairs that had decreased values of p[1] and p[2] in the loadings plot (Fig. 2B) were presumably suppressed in their formation and/or urinary excretion due to the administration of arecoline 1-oxide, also by unknown mechanisms.

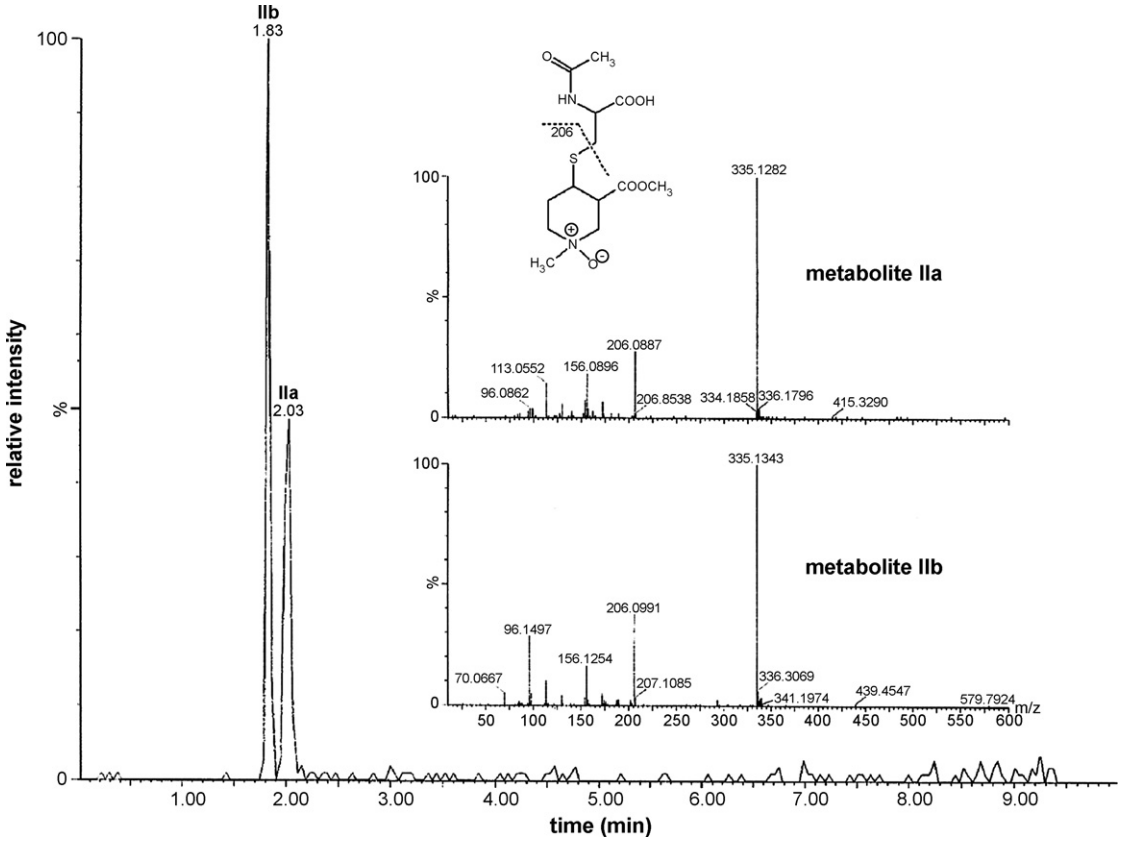

Fig. 3 – Single ion chromatogram (*m/z* 335.13) and MS/MS fragmentation of metabolites IIa and IIb.

3.2. *Identity of the urinary metabolites of (±)-arecoline 1-oxide apparent from the metabolomic analysis*

3.2.1. *Arecoline 1-oxide (I)*

The parent compound ($C_8H_{13}NO_3$) was identified from three ions of *m/z* 172.096, 343.184, and 173.102 with coincident retention times (1.12–1.13 min). Matches of these masses to the empirical formula of arecoline 1-oxide (I) were made with errors of 4.6–6.1 ppm. We have previously reported these ions, that correspond to MH^+, M_2H^+ (the protonated dimer), and the $(M + 1)H^+$ isotope ions, in a study of the metabolomics of arecoline in the mouse [6]. Moreover, the retention time of arecoline in the previous study was 1.16–1.17 min. Treatment of the urines with $TiCl_3$ caused these three ions to disappear. No further characterization of the parent compound was deemed necessary.

3.2.2. *Arecoline 1-oxide mercapturic acid diastereomers (IIa and IIb)*

Two ions of identical *m/z* (335.126), eluting at 1.83 and 2.03 min were determined to have the empirical formula of $C_{13}H_{22}N_2O_6S$ with an error of 1.2 ppm. We had previously reported this as a single ion with a retention time of 1.99 min after the administration of arecoline [6]. This empirical formula was assigned to arecoline 1-oxide mercapturic acid, but in the present study two such compounds were excreted in urine. Inspection of the structure of this compound reveals asymmetry at positions *C*3 and *C*4, meaning that arecoline 1-oxide mercapturic acid exists as two pairs of diastereomers, 3-(*R*), 4-(*S*) and 3-(*S*), 4-(*R*) [both *cis*-] together with 3-(*R*), 4-(*R*) and 3-(*S*), 4-(*S*) [both *trans*-]. It is expected therefore that two diastereomer peaks may be resolved by UPLC. These fully resolved peaks are labeled IIa and IIb in Fig. 3. Tandem mass spectrometry (MS/MS) revealed two virtually identical fragmentation patterns for IIa and IIb, both with a loss of 129 Da from the protonated molecular ion (MH^+) due to a C–S bond scission that is characteristic of mercapturic acids [18]. Moreover, these two peaks disappeared after treatment of the urines with $TiCl_3$.

3.2.3. *1-Methyl-3,4-dehydropiperidine-3-carboxaldehyde (III)*

A single ion of *m/z* 126.091 and retention time 0.58 min was observed in the contributions table from SIMCA-P+ that corresponded to an empirical formula of $C_7H_{11}NO$ with an error of 7.1 ppm. This appeared to be the second biggest contributor (Table 1) to the group differences in the PCA (Fig. 2A). MS/MS demonstrated a large stable protonated molecular ion with a single fragment ion of *m/z* 98 (Fig. 4) corresponding to a neutral loss of CO (28 Da). This confirms the structure of the aldehyde of arecoline for which the MH^+ ion is stable due to the conjugation between the carbonyl group and the 3,4-alkene, and the fragmentation follows an expected pattern for an aldehyde.

3.2.4. *1-Methylnipecotic acid 1-oxide methyl ester diastereomers (IVa and IVb)*

Two ions of identical *m/z* (174.112) were found at retention times 1.73 and 3.40 min in the contributions table and

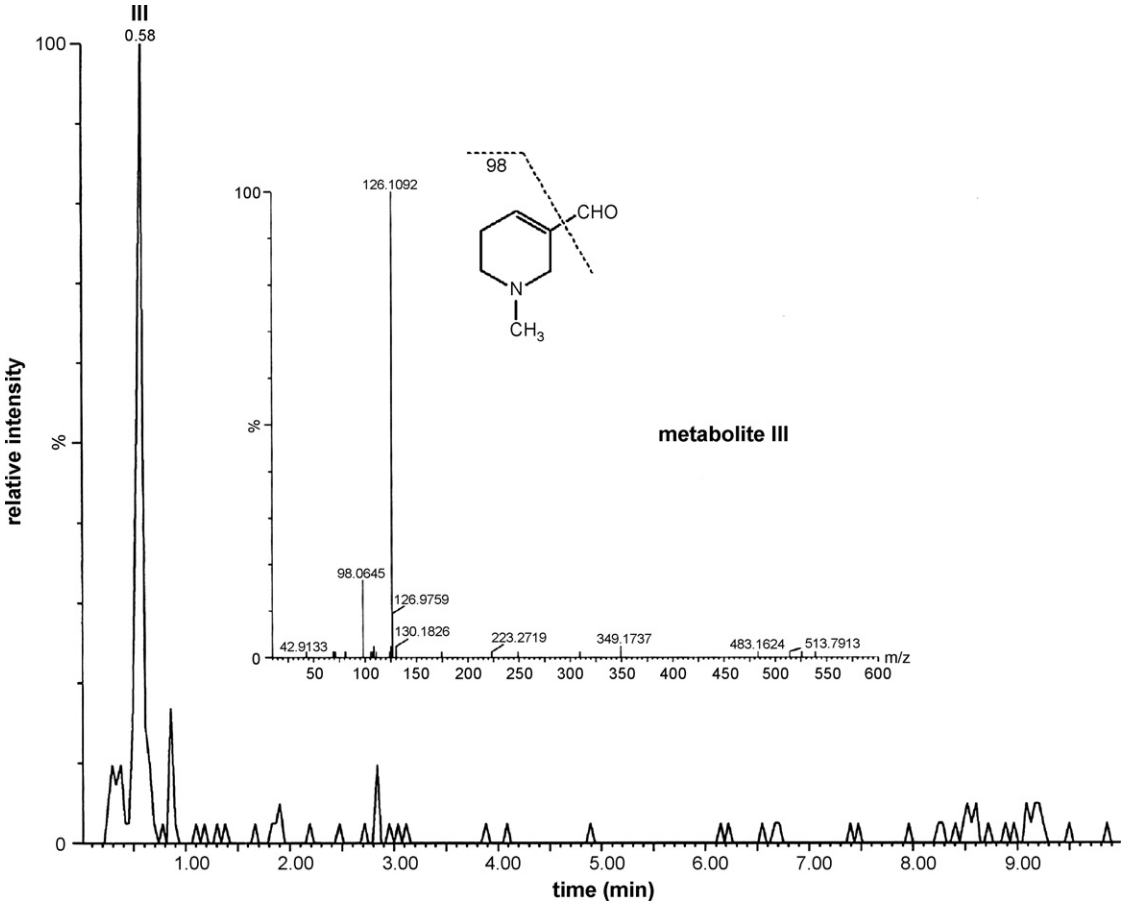

Fig. 4 – Single ion chromatogram (*m/z* 126.09) and MS/MS fragmentation of metabolite III.

corresponded to an empirical formula of $C_8H_{15}NO_3$ with an error of 2.9 ppm (Table 1). Fig. 5A shows the difference in polarity of the two peaks as judged by their disparate elution from the UPLC column. The two peaks also yielded quite different MS/MS fragmentations, with IVa having a relatively unstable protonated molecular ion and IVb demonstrating much less fragmentation of MH^+ (Fig. 5B). These two isomeric peaks were assigned the structure of 1-methylnipecotic acid 1-oxide methyl ester, a metabolite arising from the reduction of the 3,4-double bond in the parent compound. Such a metabolic reaction was also reported for the biotransformation of arecoline to 1-methylnipecotic acid in the mouse [6]. Perusal of the structure of 1-methylnipecotic acid 1-oxide methyl ester reveals chiral centers at positions N1 and C3 (Fig. 5C) and thus, the possibility of diastereomers (cf. metabolites IIa and IIb, above). The two *trans*-diastereomers are 1-(*R*), 3-(*R*) and 1-(*S*), 3-(*S*) and the *cis*-diastereomers are 1-(*R*), 3-(*S*) and 1-(*S*), 3-(*R*) [*cis*/*trans* relative to the oxide]. In the case of both *cis*-diastereomers, intramolecular hydrogen bonding is possible and likely between the protonated 1-oxide and the 3-carbonyl group, forming a secondary ring that stabilizes the protonated molecular ion. The MS/MS of the *cis* compounds is characterized by a simple loss of 17 Da from the oxide, which is typical of tertiary *N*-oxides [19]. By contrast, in the case of both *trans*-diastereomers, intramolecular interaction between the protonated 1-oxide and the ester side-chain is not feasible and it is proposed that the resultant MH^+ fragments as shown in Fig. 5C. These peaks disappeared on treatment of the urines with $TiCl_3$.

3.2.5. *4-Mercapto-1-methylnipecotic acid methyl ester diastereomers (Va, Vb, and Vc)*

Three ions of similar *m/z* (190.092, 190.096, and 190.107) were found in the contributions table at retention times 0.82, 1.95, and 2.15, respectively (Table 1). Fig. 6 shows the presence of a fourth peak of identical mass at 2.47 min, but this was not associated with arecoline 1-oxide administration in the metabolomic analysis, and was thus ignored. These masses corresponded to an empirical formula of $C_8H_{15}NO_2$ with an error of 7.4 ppm. The MS/MS revealed three different fragmentation patterns for Va, Vb, and Vc (Fig. 6). As for metabolites IIa and IIb (Fig. 3), chirality at C3 and C4 dictated the existence of diastereomers. The *cis*-diastereomers are 3-(*S*), 4-(*R*) and 3-(*R*), 4-(*S*) and the *trans*-diastereomers are 3-(*R*), 4-(*R*) and 3-(*S*), 4-(*S*). Only in the case of the *cis* compounds is intramolecular interaction probable, and thus it is proposed that the protonated carboxyl group of the MH^+ interacts with the thiol proton to eliminate H_2O (18 Da) for the *cis* isomers only (Fig. 6, mechanism not shown). Neutral loss of H_2O from protonated carboxyl groups has been studied in detail with the dipeptide GlyGly [20]. In the case of the *trans* isomers, where such intramolecular neutral loss of H_2O is less likely, it is proposed that a typical neutral loss of CH_3SH occurs (48 Da) from C4, as has been reported for *S*-methylcysteine [21]. When

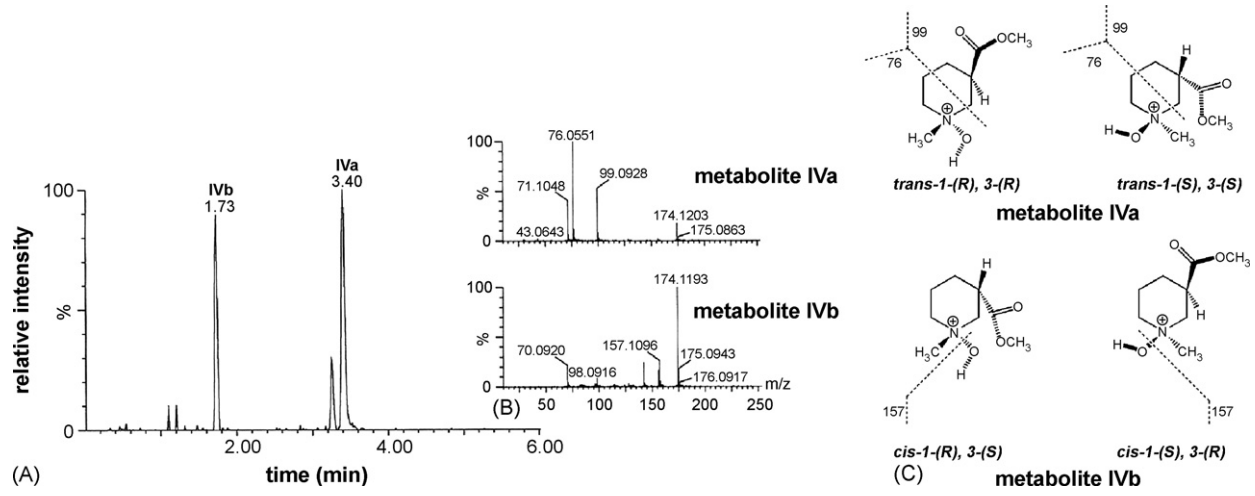

Fig. 5 – Single ion chromatogram (*m/z* 174.11) (A), MS/MS fragmentation patterns (B) and proposed fragmentation reactions (C) for metabolites IVa and IVb.

the molecular ion is protonated at N1, it should be pointed out that this introduces a third center of asymmetry with yet further possibilities of diastereoisomerism. It is therefore proposed that metabolite Va is a *trans* isomer that eliminates CH_3SH, and that metabolites Vb and Vc represent *cis* isomers that eliminate H_2O from MH^+ (Fig. 6). The presence of more than two peaks may be due to protonation of N1 in the formic acid buffer of the UPLC solvent, creating three chiral centers pre-column.

3.2.6. *Arecaidine (VI)*

A single ion of *m/z* 142.081 with a retention time of 0.30 min corresponded to a metabolite of empirical formula of $C_7H_{11}NO_2$ with an error of 8.4 ppm (Table 1). This corresponded to arecaidine (VI), the de-esterified metabolite of arecoline (VII) that we have previously reported to have a retention time of 0.28–0.30 min in our UPLC system [6]. No further characterization of this simple metabolite was necessary.

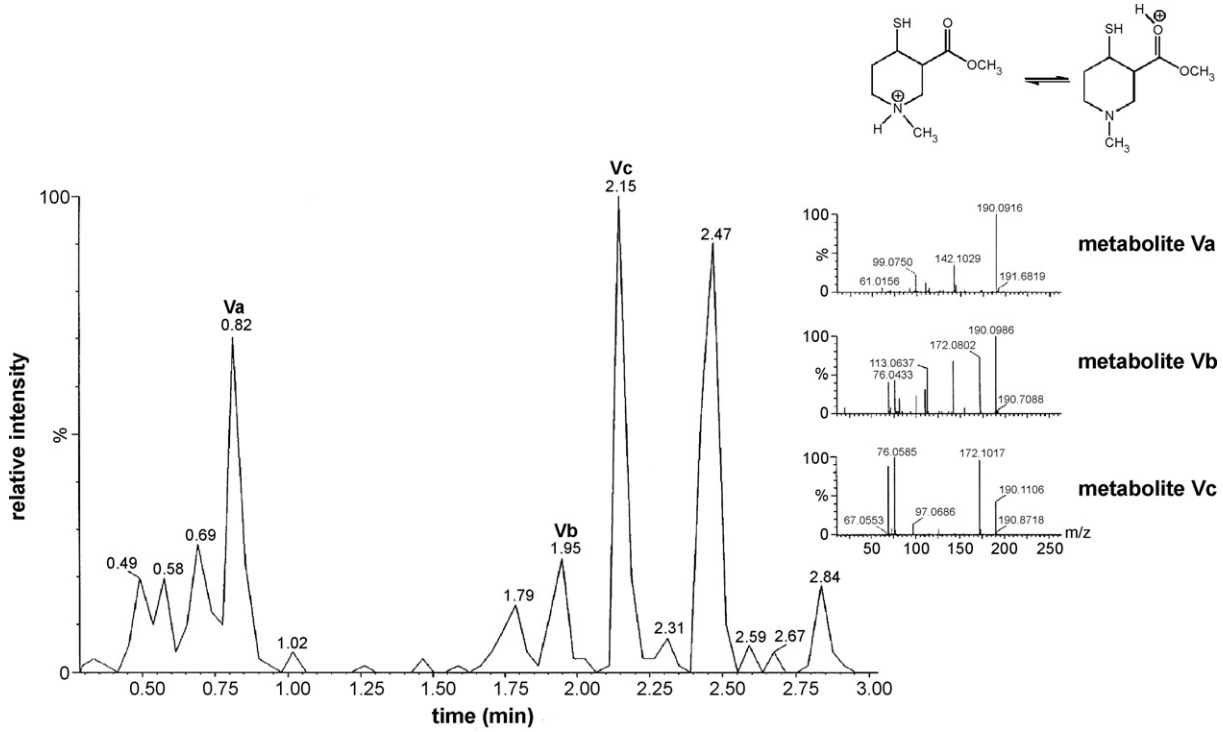

Fig. 6 – Single ion chromatogram (*m/z* 190.09) and MS/MS fragmentation of metabolites Va, Vb and Vc. Also shown are two possible protonated molecular ions.

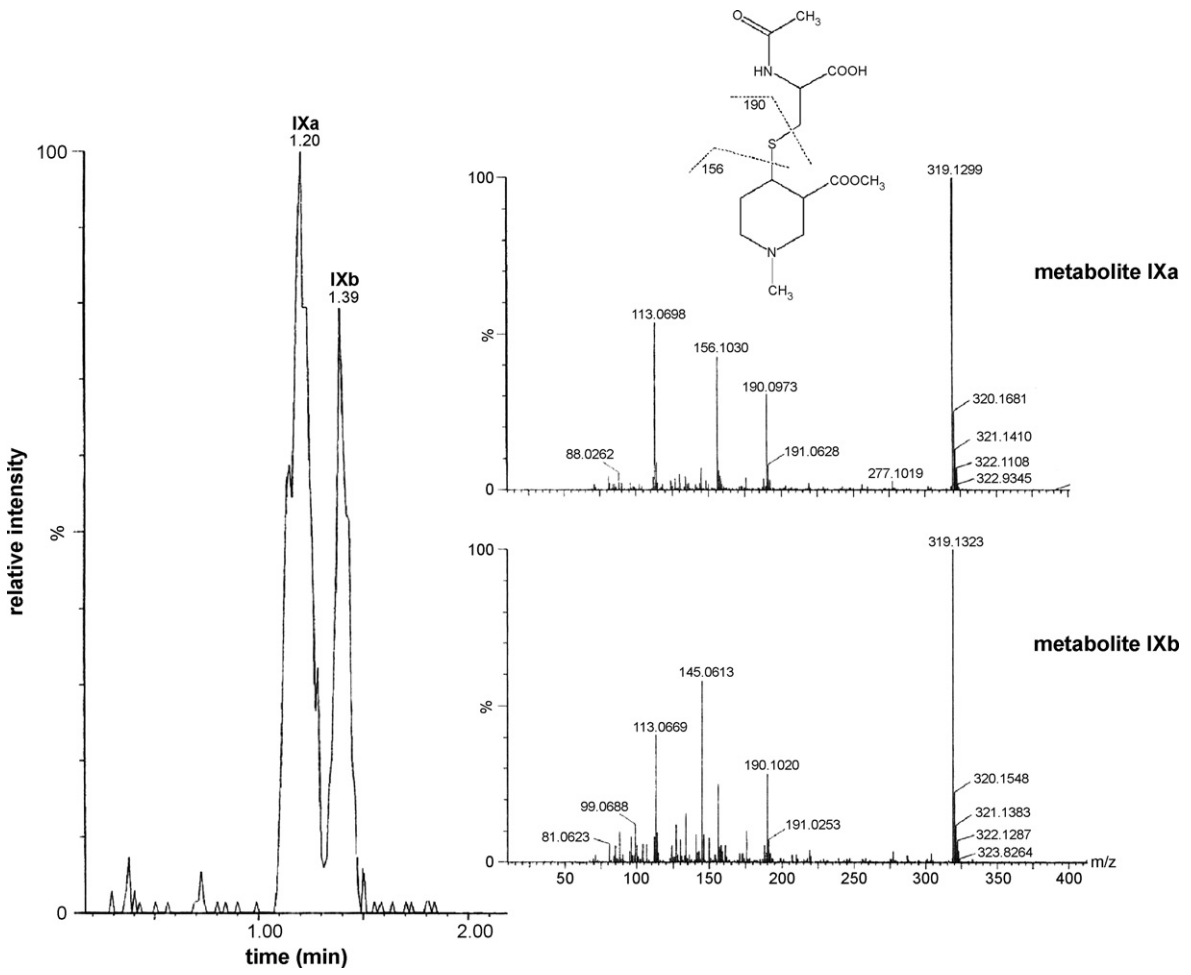

Fig. 7 – Single ion chromatogram (*m/z* 319.13), MS/MS fragmentation patterns and proposed fragmentation reactions for metabolites IXa and IXb.

3.2.7. *4-Methylmercapto-1-methylnipecotic acid 1-oxide methyl ester (VII)*

A single ion of *m/z* 220.101 and retention time 2.38 min appeared in the contributions table. This was assigned to a metabolite with an empirical formula of $C_9H_{17}NO_3S$ with an error of 2.7 ppm and corresponded to the product of cysteine S-conjugate β-lyase activity [22] on the mercapturic acids (IIa and IIb) of the parent compound. It is also the likely precursor of the thiol metabolites (Va, Vb, and Vc). It is not known why diastereomers arising from chirality at C3 and C4 did not appear as chromatographically resolved biomarkers in the metabolomic analysis. This peak disappeared on the treatment of the urines with $TiCl_3$. No further characterization of this metabolite was performed.

3.2.8. *Arecoline (VIII)*

A single ion with *m/z* of 156.102 and retention time of 0.64 min corresponded to a metabolite with an empirical formula of $C_8H_{13}NO_2$ with an error of 5.8 ppm (Table 1). We have previously reported that arecoline eluted in this UPLC system at 0.63 min [6]. This metabolite results from the *N*-oxide reduction of the parent compound (I). No further characterization of this metabolite was deemed necessary.

3.2.9. *Arecoline mercapturic acid diastereomers (IXa and IXb)*

Two ions of identical *m/z* (319.133) eluted at 1.26 and 1.41 min. They gave an empirical formula of $C_{13}H_{22}N_2O_5S$ with an error of 5.3 ppm. We have previously reported this as a metabolite of arecoline in the mouse with a retention time of 1.22–1.23 [6] and this formula corresponds to two diastereomeric arecoline mercapturic acids (IXa and IXb in Fig. 7). As with other metabolites described above, chirality at C3 and C4 leads to diastereomers. Fig. 7 shows that the two diastereomeric mercapturic acids are almost completely resolved by UPLC. Both metabolites display the typical neutral loss of 129 Da [18]. Interestingly, metabolite IXa displays a further neutral loss of H_2S (34 Da), while metabolite IXb loses 44 Da, which may represent the elimination of CO_2 from the ester side-chain.

Thus, unchanged arecoline 1-oxide has been identified in mouse urine, together with 13 metabolites, including chromatographically-resolved diastereomers. This corresponds to the occurrence of five primary and four secondary metabolic pathways in the mouse after the administration of (±)-arecoline 1-oxide. In order to visualize better these biotransformations, a metabolic map for (±)-arecoline 1-oxide in the mouse is shown in Fig. 8. The relative importance of each pathway will be dealt with below.

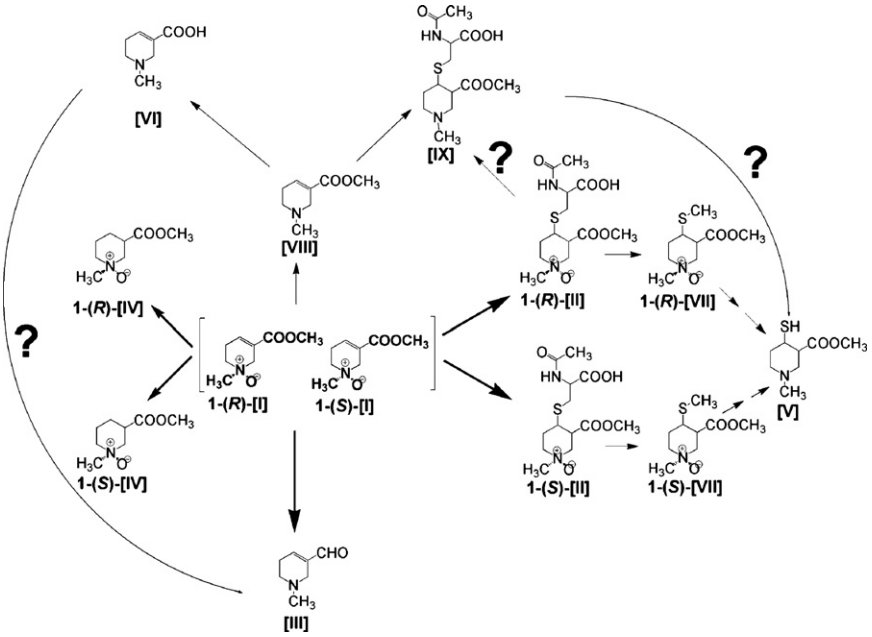

Fig. 8 – The metabolic map of (±)-arecoline 1-oxide in the mouse. Major pathways are depicted with darker arrows. The annotation "?" denotes alternative pathways.

3.3. *Quantitation of the urinary metabolites of (±)-arecoline 1-oxide apparent from the metabolomic analysis*

3.3.1. *Estimation of relative concentrations of metabolites by metabolomic analysis*

Table 1 displays a score value that derives from the metabolomic analysis and is a function of the contribution of each individual metabolite (ion/retention time pair) to the group separation between test and control urines displayed in the PCA scores plot (Fig. 2A). The values of this score range from 41.9 for the parent compound, with the other metabolites having values in the range 2.8–6.7 (Table 1). It is proposed here that these metabolomic scores are a function of the relative concentration of individual metabolites, as will be established below. This analysis would suggest that (±)-arecoline 1-oxide (20 mg/kg p.o.) administration to the mouse results in approximately 50% of the 0–24 h urinary metabolites comprising unchanged parent compound. This proposition will be further tested below.

3.3.2. *Estimation of relative concentrations of metabolites by chromatographic analysis*

Table 1 also displays the areas of randomly selected peaks derived from UPLC chromatograms of extracted exact masses at 50 ppm tolerance, such as those shown in Figs. 3–7. These data also suggest that (±)-arecoline 1-oxide is excreted at least 50% unchanged in urine after administration to mice. As mentioned earlier, three assumptions have been made: (i) that all compounds under investigation ionize to a similar extent in the ES+ mode, (ii) that there is little or no in-source fragmentation that would limit the yield of MH^+ ions, and (iii) that ion suppression effects are equivalent over the first 3.5 min of the chromatogram, the period in which all the metabolites in Table 1 eluted. Our experience with both MS and MS/MS modes, together with voltage adjustments, assure us that these assumptions are reasonable. In addition, all metabolites listed in Table 1 are polar and contain readily protonatable functional groups, such as ≡N→O and >C═O. To test these various assumptions further, a correlation was performed between the metabolomic scores and the chromatographic peak areas. The results are shown in Fig. 9. The regression in Fig. 9A is highly significant ($r = 0.99$, $P < 0.001$). However, the correlation is skewed and invalidated by one single high point that corresponds to the parent compound (m/z 172.096). Therefore, this value was eliminated and the data recorrelated and shown in Fig. 9B. As can be seen, there is still a linear positive and highly statistically significant ($r = 0.90$, $P = 0.009$) correlation between the metabolomic score and the chromatographic peak area. These data also show that metabolomic scores <3 may not provide meaningful insights into the relative proportions of metabolites in urine. Therefore, the value of 3 has been set as a threshold (Fig. 9).

For the purposes of comparison of relative amounts of each metabolite in urine, the metabolomic score was used. This had the added benefit of being a single number which represented the effect of the individual ion/retention time pair on the group separation between blank and test urines. The relative percent of each urinary metabolite is displayed in Fig. 10. Approximately, half of the excreted material comprises unchanged arecoline 1-oxide. Three other *N*-oxides comprised a further 28.6% of the urinary metabolites. Thus, about 80% of the metabolites in urine retained the intact *N*-oxide group. The principal metabolites were the mercapturic acids (IIa and IIb) of the parent compound, the nipecotic acid 1-oxide methyl esters (IVa and IVb) arising from C═C bond reduction, and the thiol metabolites (Va–Vc) derived from the further metabolism of the mercapturic

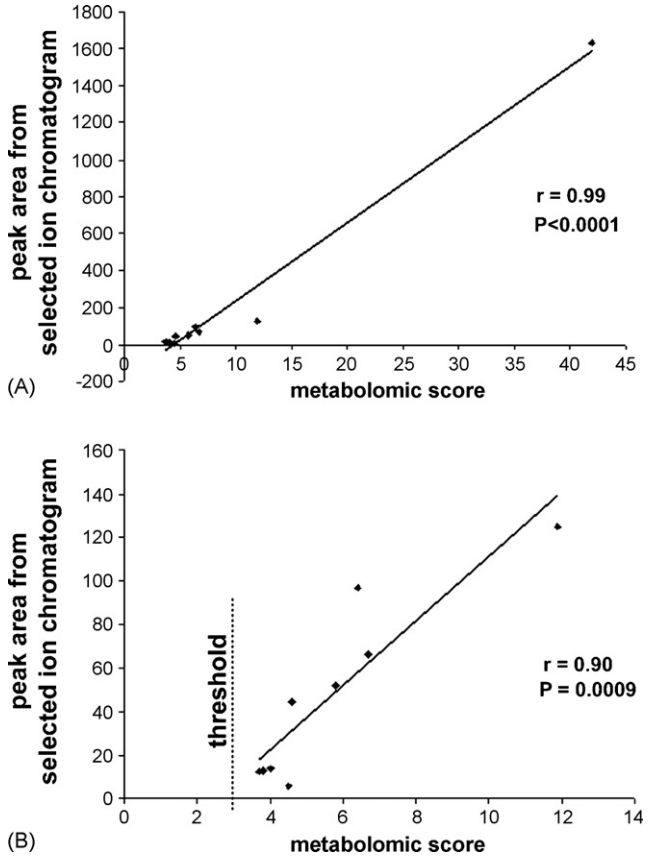

Fig. 9 – Correlation between the metabolomic score and chromatographic peak areas, with (A) and without (B) inclusion of the outlying ion 172.096$^+$ (parent compound).

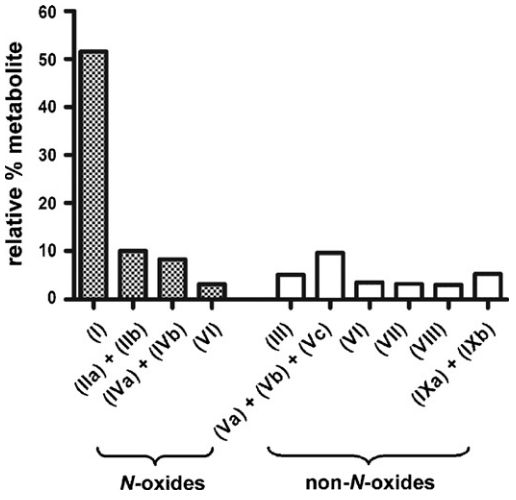

Fig. 10 – Relative proportion of individual urinary metabolites of (±)-arecoline 1-oxide in the mouse. Stippled bars represent N-oxide metabolites and open bars metabolites where the N-oxide has been reduced.

acids. In addition, 34.7% of the metabolites (IIa, IIb, IVa, IVb, VII, IXa, and IXb) could be directly attributed to mercapturic acid formation.

3.4. *N*-Oxidation of arecoline by recombinant human P450 isozymes

None of the 11 recombinant human P450s tested (CYP1A1, CYP1A2, CYP1B1, CYP2A6, CYP2B6, CYP2C9, CYP2C19, CYP2D6, CYP2E1, CYP3A4, and CYP4A11) *N*-oxidized arecoline (50 μM).

3.5. *N*-Oxidation of arecoline by recombinant human FMO isozymes

Under the conditions of the experiments at pH 7.9 and a concentration of 50 μM arecoline, only FMO1 and FMO3 produced arecoline 1-oxide *in vitro*. When pH 7.4 tris–HCl buffer was substituted for pH 7.9 potassium phosphate buffer, *N*-oxidation was reduced to 84% for FMO1 and to 37% for FMO3. When pH 9.0 glycine buffer was used, *N*-oxidation was reduced to 38% for FMO1 and to 21% for FMO3, compared with pH 7.9. In all cases where product was formed *in vitro*, the identity of arecoline 1-oxide was confirmed not only from the selected ion chromatogram (*m/z* 172.098, 50 ppm tolerance), but also by MS/MS experiments that produced fragmentation patterns identical to authentic arecoline 1-oxide. Accordingly, further experiments were performed to investigate the relative importance of FMO1 and FMO3 in arecoline *N*-oxidation. Firstly, it was established that arecoline *N*-oxidation by both FMO1 and FMO3 was linear with respect to enzyme concentration (0–200 nM; data not shown). Secondly, it was established that the rate of arecoline *N*-oxidation by FMO1 was linear up to 20 min and by FMO3 was linear up to 25 min. The specificity of the reactions were checked by using the FMO inhibitor methimazole at 10, 100, 200, and 1000 μM. The reaction with FMO1 was >90% inhibited at 1000 μM methimazole, with an IC_{50} value of ~90 μM. The reaction with FMO3 was completely inhibited at 100 μM methimazole (data not shown).

3.6. Michaelis–Menten kinetics of arecoline *N*-oxidation by FMO1 and FMO3

The calibration curve for arecoline 1-oxide determination by UPLC-TOFMS using caffeine as internal standard was linear from 0 to 50 μM arecoline 1-oxide ($r = 0.995$). The velocity (V) versus substrate concentration (S) curve for *N*-oxidation by both FMO1 and FMO3 is shown in Fig. 11A and the Lineweaver–Burk reciprocal plots are shown in Fig. 11B. From these data it was determined that the K_M estimates (mean ± S.D.) for FMO1 and FMO3 were 13.6 ± 4.9 and 44.5 ± 8.0 μM, respectively, and the V_{max} estimates for FMO1 and FMO3 were 0.114 ± 0.01 and 0.014 ± 0.001 nmol min^{-1} μg^{-1} FMO. These values yielded intrinsic clearances (V_{max}/K_M) for FMO1 and FMO3 of 8.4 and 0.32 ml min^{-1} μg^{-1} enzyme, respectively, $a > 25$-fold difference between FMO1 and FMO3. The *N*-oxidation of arecoline appears to be preferentially carried out by the renal isozyme FMO1 and to a lesser extent by the hepatic isozyme FMO3, although it is the relative abundance of each isozyme that will determine which isozyme is preferentially utilized in any given tissue.

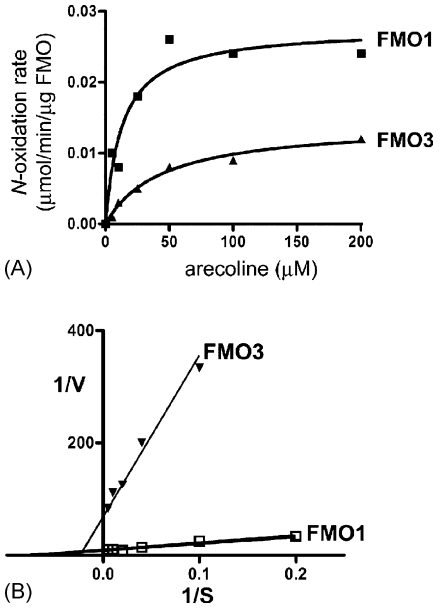

Fig. 11 – Velocity curves for the N-oxidation of arecoline by human FMO1 and FMO3 (A) and the Lineweaver–Burk reciprocal plots for human FMO1 and FMO3 (B).

4. Discussion

Metabolomic methodologies, the fusion of a high-resolution technology such as UPLC (resolving 5000 protonated ions in a 9 min chromatogram), with exact mass determination by TOFMS, and MVA using SIMCA-P+, provide a new horizon in drug metabolism studies. We have recently reported the identification of 11 metabolites of the areca nut alkaloid arecoline [6] and 13 metabolites of the experimental anticancer drug Aminoflavone [23] using this approach to analyze mouse urine. The majority of the metabolites described were novel. Secondary MS/MS experiments were used to confirm the identity of metabolites. In this report, we have studied one of the two major urinary metabolites of arecoline in the mouse, (±)-arecoline 1-oxide after oral administration (20 mg/kg) and demonstrated its biotransformation by mercapturic acid formation and further derivatives, ester hydrolysis, *N*-oxide reduction, C=C double-bond reduction, carboxylic acid (ester) reduction to the aldehyde, together with various combinations of these pathways. Furthermore, four of these metabolites were detected as diastereomers, making a total of 14 urinary metabolites, including the parent compound. Only a sketchy account of the administration of arecoline 1-oxide to two rats has been reported and the author assumed that *N*-oxide reduction back to arecoline was the hallmark of its metabolism [8]. The great majority of the metabolites of (±)-arecoline 1-oxide reported here are novel.

A unique method for estimation of the relative concentrations of each metabolite in urine has been employed, using scores for individual ion/retention time pairs derived from the metabolomic analysis. These metabolomic scores correlated well with the peak areas obtained from the selected ion chromatograms (Fig. 9). By making three basic assumptions about the equivalency of ionization and gas phase stability of ions throughout the chromatographic run, the metabolomic score was employed here as a tool for metabolite quantitation. Further validation of this approach using known concentrations of authentic compounds in urine will be required before the metabolomic score can be used more generally. Nevertheless, this variable has furnished important insights into the murine biotransformation and urinary excretion of (±)-arecoline 1-oxide. A metabolic map has been constructed (Fig. 8) which, in combination with the quantitative data (Fig. 10), has opened a window on the metabolic behavior of (±)-arecoline 1-oxide in the mouse. First, it would appear that approximately half of the drug-related material in urine comprises unchanged compound. However, there is evidence that *N*-oxides may undergo metabolic reduction *in vivo*, perhaps by the gut flora, before being *N*-oxidized back to the parent compound. It was possible to visualize this process, termed ''metabolic retroversion'', by administration of trimethylamine *N*-oxide (TMAO) to two persons with an inherited trimethylamine *N*-oxidation deficiency, known as fish-odor syndrome. While unaffected subjects excreted >94% of the administered TMAO apparently unchanged, with only 4% as the free base trimethylamine (TMA), the two affected patients excreted 35 and 51% of dose as TMA, and two heterozygous subjects excreted 12 and 16% of dose as TMA. Overall, these findings suggested that 40–60% of an oral dose of TMAO undergoes retroverted metabolism [9]. In addition to the observation of arecoline excretion after arecoline 1-oxide administration to rats [8], administration of either arecoline [6] or (±)-arecoline 1-oxide (Table 1; Figs. 8 and 10) both lead to the excretion of arecoline 1-oxide, arecoline, arecaidine, arecoline mercapturic acid, and arecoline 1-oxide mercapturic acid. It is therefore possible that (±)-arecoline 1-oxide undergoes an unknown degree of metabolic retroversion and that, as has been claimed [8], the metabolites of the 1-oxide originate via arecoline. However, this prospect appears unlikely in the most part, because ~80% of the urinary metabolites are *N*-oxides (Fig. 10).

The range and possible interconversion of urinary metabolites of (±)-arecoline 1-oxide are worthy of comment. Fig. 8 shows a metabolic map for which metabolism depicted in the horizontal plane is that which retains the *N*-oxide, specifically mercapturic acid formation and C=C double-bond reduction. Both of these pathways occur also for arecoline [6] and, moreover, the latter reaction (alkene reduction) is without precedent in mammalian drug metabolism. However, a major distinction must be made between the reductive reaction for arecoline and for its *N*-oxide. In the case of arecoline, the finding was of urinary *N*-methylnipecotic acid, the reduced product of the primary metabolite arecaidine. Accordingly, it was suggested that the reduction occurred via a CoA-dependent pathway, possibly by *trans*-2-enoyl thioester reductase (EC 1.3.1.38) [6]. In the case of the *N*-oxide reported here, this mechanism would not be feasible, since the reduced metabolites (IVa and IVb) retain the methyl ester group. An alternative mechanism must be sought. The clues perhaps arise from the apparent ready formation of mercapturic acids (IIa, IIb, and VII) from the *N*-oxide and their subsequent methylmercaptan and mercaptan derivatives (Va–c and VII), which together account for some 30% of the urinary

metabolites of (±)-arecoline 1-oxide. In all these metabolites, the C=C double-bond has been "reduced" by the addition of the endogenous thiol, be it GSH, cysteine or *N*-acetylcysteine. Metabolic scission of the heterocycle-sulfur bond would lead to the observed metabolites, both in the case of (±)-arecoline 1-oxide and arecoline. To our knowledge, such a metabolic reaction for mercapturic acids, or for glutathione conjugates, has not been described.

Fig. 8 also displays in the vertical plane metabolic pathways of (±)-arecoline 1-oxide for which the *N*-oxide has been metabolically reduced. The most significant of these is the carboxaldehyde derivative (III) of arecoline. Interestingly, this metabolite, which represents the loss of a single atom of oxygen from arecaidine (VI), was not detected after the administration to mice of either arecoline or arecaidine [6], suggesting that it is formed from the *N*-oxide without prior reduction to arecoline and arecaidine. Both metabolic options are depicted in Fig. 8. A carboxylic acid reductase has been reported in bacteria and fungi [24,25] that can metabolize benzoic, vanillic and ferulic acids to their corresponding aldehydes [25]. Although this is an analogous pathway as described herein, this aldehyde oxidoreductase activity [25] has not been reported to occur in mammals. This provides evidence for a role of the gut flora in arecoline 1-oxide metabolism. In humans, the intestinal microbiota contains at least 100 times as many genes as the human genome [26] and therefore is an important source of xenobiotic metabolism.

The formation or arecoline (VIII) by *N*-oxide reduction has been previously reported [8] and this presumably is the precursor for the observed arecaidine (VI) by ester hydrolysis and for the diastereomeric arecoline mercapturic acids (IXa and IXb). However, these mercapturic acids may be formed by *N*-oxide reduction of the corresponding arecoline 1-oxide mercapturic acids (IIa and IIb). Both pathways are depicted in Fig. 8. Finally, the question arises whether the mercaptan metabolites (Va–c) are formed in a two-step reaction from the observed methylmercaptan metabolite (VII), or whether by the action of cysteine *S*-conjugate β-lyase [22] on arecoline mercapturic acids (IXa and IXb). Again, both pathways are depicted in the metabolic map. A clearer understanding of these interconversions would only be possible from investigations that administered the individual enantiomers of arecoline 1-oxide (Fig. 1).

This report has furnished a much clearer picture of the metabolic transformations of (±)-arecoline 1-oxide. Taken together with the metabolic map of arecoline and arecaidine [6], these new data may be helpful in dissecting the biochemical and cellular components of the clinical toxicology of areca nut chewing. This habit has some 600 million devotees [1,2] and is associated with several public health concerns [3–5], including oral cancer [3,5]. The mechanisms of carcinogenesis of the areca alkaloids are not known, although several nitrosamines derived from these alkaloids have been the suspected agents. Notwithstanding, these nitrosamines display little or no mutagenicity or carcinogenicity in model systems. Alternative mechanisms should conceivably be sought. For example, arecoline readily undergoes a direct chemical reaction with *N*-acetylcysteine, which is the basis of the chemical synthesis of its mercapturic acid [7]. It is possible that the same reaction occurs *in vivo*, without the intervention of a glutathione *S*-transferase enzyme. Direct reaction with cellular thiols might therefore occur in tissues with low levels, or lacking, glutathione *S*-transferases, such as the buccal mucosa. Elevated local concentrations of areca alkaloids, such as arecoline and arecaidine, might therefore reduce cellular thiols in oral tissues and thus, impair anti-oxidant defenses, perhaps leading to alkylation of tissue macromolecules once these defenses had been overcome. Detailed knowledge of the metabolism of these alkaloids would be expected to contribute to our understanding of the clinical toxicology of areca nut chewing.

In summary, a metabolomic approach to the metabolism of (±)-arecoline 1-oxide in the mouse has led to a better understanding of the metabolic map for both (±)-arecoline 1-oxide and its precursor alkaloid arecoline. Several novel metabolites, many formed as diastereomers, have been revealed by this unique approach. Additionally, metabolic pathways hitherto not described in mammals were also observed, including carboxylic acid reduction and C=C double-bond reduction. Approximately, 50% of the urinary metabolites comprised unchanged parent compound, with a further 20% as other *N*-oxide derivatives. Several mercapturic acids and their catabolic products were observed, comprising some 30% of the urinary metabolites of (±)-arecoline 1-oxide. Arecoline 1-oxide was demonstrated not to be formed by a panel of human P450s, but was formed by both FMO1 and FMO3, the intrinsic clearance (V_{max}/K_M) of the former being over 25-times the later. These data suggest that arecoline may be converted to its *N*-oxide in human tissues other than the liver, especially the kidney, where FMO1 is predominantly expressed [12,13]. These data may point to a role for the kidney in the human pharmacology and toxicology of the areca alkaloids.

Acknowledgements

The authors are grateful to Dr. Mark Zabriskie, Oregon State University, for the determination of specific optical rotation of synthetic arecoline 1-oxide. Supported by the National Cancer Institute Intramural Research Program of the NIH. J.R.I. is grateful to U.S. Smokeless Tobacco Company for a grant for collaborative research. S.G. was the recipient of a DBT Overseas Associateship (# BT/IN/BTOA/18/2004) from the Department of Biotechnology, Ministry of Science and Technology, Government of India.

REFERENCES

[1] Gupta PC, Warnakulasuriya S. Global epidemiology of areca nut usage. Addict Biol 2002;7(1):77–83.
[2] Winstock A. Areca nut-abuse liability, dependence and public health. Addict Biol 2002;7(1):133–8.
[3] IARC. Betel-quid and areca-nut chewing and some areca-nut-derived nitrosamines, vol. 85. Lyon: IARC; 2004.
[4] Bhargava K, Smith LW, Mani NJ, Silverman Jr S, Malaowalla AM, Bilimoria KF. A follow up study of oral cancer and precancerous lesions in 57,518 industrial workers of Gujarat, India. Indian J Cancer 1975;12(2):124–9.

[5] Warnakulasuriya S, Trivedy C, Peters TJ. Areca nut use: an independent risk factor for oral cancer. Br Med J 2002;324(7341):799–800.
[6] Giri S, Idle JR, Chen C, Zabriskie TM, Krausz KW, Gonzalez FJ. A metabolomic approach to the metabolism of the areca nut alkaloids arecoline and arecaidine in the mouse. Chem Res Toxicol 2006;19(6):818–27.
[7] Boyland E, Nery R. Mercapturic acid formation during the metabolism of arecoline and arecaidine in the rat. Biochem J 1969;113(1):123–30.
[8] Nery R. The metabolic interconversion of arecoline and arecoline 1-oxide in the rat. Biochem J 1971;122(4):503–8.
[9] Al-Waiz M, Ayesh R, Mitchell SC, Idle JR, Smith RL. Disclosure of the metabolic retroversion of trimethylamine N-oxide in humans: a pharmacogenetic approach. Clin Pharmacol Ther 1987;42(6):608–12.
[10] Ziegler DM. Recent studies on the structure and function of multisubstrate flavin-containing monooxygenases. Annu Rev Pharmacol Toxicol 1993;33:179–99.
[11] Guengerich FP, Vaz AD, Raner GN, Pernecky SJ, Coon MJ. Evidence for a role of a perferryl-oxygen complex, FeO_3^+, in the N-oxygenation of amines by cytochrome P450 enzymes. Mol Pharmacol 1997;51(1):147–51.
[12] Cashman JR, Zhang J. Human flavin-containing monooxygenases. Annu Rev Pharmacol Toxicol 2006;46: 65–100.
[13] Zhang J, Cashman JR. Quantitative analysis of FMO gene mRNA levels in human tissues. Drug Metab Dispos 2006;34(1):19–26.
[14] Selvan RS, Selvakumaran M, Rao AR. Influence of arecoline on immune system: II. Suppression of thymus-dependent immune responses and parameter of non-specific resistance after short-term exposure. Immunopharmacol Immunotoxicol 1991;13(3):281–309.
[15] Parte P, Kupfer D. Oxidation of tamoxifen by human flavin-containing monooxygenase (FMO) 1 and FMO3 to tamoxifen-N-oxide and its novel reduction back to tamoxifen by human cytochromes P450 and hemoglobin. Drug Metab Dispos 2005;33(10):1446–52.
[16] Wilson ID, Nicholson JK, Castro-Perez J, Granger JH, Johnson KA, Smith BW, et al. High resolution ''ultra performance'' liquid chromatography coupled to oa-TOF mass spectrometry as a tool for differential metabolic pathway profiling in functional genomic studies. J Proteome Res 2005;4(2):591–8.
[17] Kulanthaivel P, Barbuch RJ, Davidson RS, Yi P, Rener GA, Mattiuz EL, et al. Selective reduction of N-oxides to amines: application to drug metabolism. Drug Metab Dispos 2004;32(9):966–72.
[18] Jones AD, Winter CK, Buonarati MH, Segall HJ. Analysis of mercapturic acid conjugates of xenobiotic compounds using negative ionization and tandem mass spectrometry. Biol Mass Spectrom 1993;22(1):68–76.
[19] Ma S, Chowdhury SK, Alton KB. Thermally induced N-to-O rearrangement of tert-N-oxides in atmospheric pressure chemical ionization and atmospheric pressure photoionization mass spectrometry: differentiation of N-oxidation from hydroxylation and potential determination of N-oxidation site. Anal Chem 2005;77(11):3676–82.
[20] Balta B, Aviyente V, Lifshitz C. Elimination of water from the carboxyl group of GlyGlyH+. J Am Soc Mass Spectrom 2003;14(10):1192–203.
[21] Reid GE, Simpson RJ, O'Hari RA. Leaving group and gas phase neighboring group effects in the side chain losses from protonated serine and its derivatives. J Am Soc Mass Spectrom 2000;11(12):1047–60.
[22] Cooper AJ. Mechanisms of cysteine S-conjugate beta-lyases. Adv Enzymol Relat Areas Mol Biol 1998;72: 199–238.
[23] Chen C, Meng L, Ma X, Krausz KW, Pommier Y, Idle JR, et al. Urinary metabolite profiling reveals CYP1A2-mediated metabolism of NSC686288 (Aminoflavone). J Pharmacol Exp Ther 2006;318(3):1330–42.
[24] White H, Strobl G, Feicht R, Simon H. Carboxylic acid reductase: a new tungsten enzyme catalyses the reduction of non-activated carboxylic acids to aldehydes. Eur J Biochem 1989;184(1):89–96.
[25] He A, Li T, Daniels L, Fotheringham I, Rosazza JP. Nocardia sp. carboxylic acid reductase: cloning, expression, and characterization of a new aldehyde oxidoreductase family. Appl Environ Microbiol 2004;70(3):1874–81.
[26] Gill SR, Pop M, Deboy RT, Eckburg PB, Turnbaugh PJ, Samuel BS, et al. Metagenomic analysis of the human distal gut microbiome. Science 2006;312(5778):1355–9.